Anal. Chem. **2009,** *81,* 3478–3484

Simple Approach for Efficient Encapsulation of Enzyme in Silica Matrix with Retained Bioactivity

Si Yang, Wen-Zhi Jia, Qing-Yun Qian, Yi-Ge Zhou, and Xing-Hua Xia*

Key Laboratory of Analytical Chemistry for Life Science, School of Chemistry and Chemical Engineering, Nanjing University, Nanjing 210093, P.R. China

We developed an alcohol-free sol−gel approach to encapsulate biomolecules such as horseradish peroxidase (HRP) in an electrochemically induced three-dimensional porous silica matrix by a one-step process. In this sol−gel process, the electrochemically generated hydroxyl ions at the electrode surface by applying cathodic current promote the hydrolysis of ammonium fluorosilicate to produce silica, and simultaneously the generated hydrogen bubbles play an important role in forming porous silica matrix. If HRP is mixed with ammonium fluorosilicate solution, it can be encapsulated in the forming silica matrix. Since there is no ethanol involved in the entire procedure, bioactivities of the encapsulated HRP can be effectively retained. As revealed by scanning electron microscopy (SEM) characterization, the resultant silica matrix has interconnected and network-like porous structures. Macroporous holes induced by hydrogen bubbles scattering on the relatively flat areas of porous structure can be observed. Such structure free from cracks provides effective mass transport and long-term stability. Scanning electrochemical microscope (SECM) characterization shows that the immobilized HRP molecules uniformly distribute in the silica matrix. The present HRP electrochemical biosensor exhibits a quick response (within 5 s) to H_2O_2 in the concentration range from 0.02 to 0.20 mM (correlation coefficient of 0.9934) with a detection limit of 3 μM. The apparent Michaelis−Menten constant is 0.88 mM. The present alcohol-free sol−gel approach is effective for biomolecule encapsulation and is promising for the construction of biosensors, bioelectronics, and biofuel cells.

Study of the sol−gel process has far-reaching influence on the development of biocatalysis, biosensors, bioelectronics, and biofuel cells because of its various outstanding advantages for biomolecule immobilization, which draws much attention of researchers.[1−5] The sol−gel process is a room temperature route and under such a condition enzymes usually can withstand. Besides, sol−gel derived materials are chemically inert, hydrophilic, and thermally stable, which can avoid the denaturation of enzymes.[6−10] Most methods used to entrap enzymes in a silica matrix are two-step processes. One of them is to mix enzymes with sol−gel precursor followed by dip-coating or spin-coating to transfer the mixture onto the surface of electrodes.[11−14] As solvent evaporates, the gelation will take place and meanwhile the biomolecules are entrapped in the silica networks. Such process suffers several disadvantages. It is time-consuming and often sol−gel matrixes derived via this method lack porosity.[15,16] The most serious problem is that alcohol is always involved in the sol−gel process as either the cosolvent or the byproduct which may denature biomolecules. Other two-step methods include physical or chemical adsorption,[17−19] which may encounter the problem of biomolecule leakage, definitely resulting in poor stability.

Our group has developed a one-step method to entrap enzyme in silica matrixes.[20] In this method, precursory sol solution is made up of glucose oxidase (GOD), tetraethyl orthosilicate (TEOS), and ethanol. After a negative potential is applied to the working electrode, reduction of water of the precursor solution alters the local pH, which in turn induces the sol−gel process to form silica matrix with GOD encapsulated simultaneously. The evolved hydrogen bubbles functioning as a kind of dynamic template help to form a porous structure;[21,22] thus, free mass transport through the matrix would not be blocked. This method is much simpler

* To whom correspondence should be addressed. E-mail: xhxia@nju.edu.cn.

(1) Sotiropoulou, S.; Chaniotakis, N. A. *Biomaterials* **2005**, *26*, 6771–6779.
(2) Kim, S.; Kim, Y.; Kim, P.; Ha, J. M.; Kim, K.; Sohn, M.; Yoo, J. S.; Lee, J.; Kwon, J. A.; Lee, K. N. *Anal. Chem.* **2006**, *78*, 7392–7396.
(3) Massari, A. M.; Finkelstein, I. J.; Fayer, M. D. *J. Am. Chem. Soc.* **2006**, *128*, 3990–3997.
(4) Wheeler, K. E.; Nocek, J. M.; Hoffman, B. M. *J. Am. Chem. Soc.* **2006**, *128*, 14782–14783.
(5) Dunn, B.; Zink, J. I. *Acc. Chem. Res.* **2007**, *40*, 747–755.
(6) Chen, Q.; Kenausis, G. L.; Heller, A. *J. Am. Chem. Soc.* **1998**, *120*, 4582–4585.
(7) Gill, I.; Ballesteros, A. *J. Am. Chem. Soc.* **1998**, *120*, 8587–8598.
(8) Pierre, A. C. *Biocatal. Biotransform.* **2004**, *22*, 145–170.
(9) Avnir, D.; Coradin, T.; Lev, O.; Livage, J. *J. Mater. Chem.* **2006**, *16*, 1013–1030.
(10) Coradin, T.; Livage, J. *Acc. Chem. Res.* **2007**, *40*, 819–826.
(11) Walcarius, A. *Electroanalysis* **1998**, *10*, 1217–1235.
(12) Pandey, P. C.; Upadhyay, S.; Pathak, H. C. *Sens. Actuators, B* **1999**, *60*, 83–89.
(13) Wang, B. Q.; Li, B.; Wang, Z. X.; Xu, G. B.; Wang, Q.; Dong, S. *J. Anal. Chem.* **1999**, *71*, 1935–1939.
(14) Iwuoha, E. I.; Kane, S.; Ania, C. O.; Smyth, M. R.; de Montellano, P. R. O.; Fuhr, U. *Electroanalysis* **2000**, *12*, 980–986.
(15) Collinson, M. M.; Rausch, C. G.; Voigt, A. *Langmuir* **1997**, *13*, 7245–7251.
(16) Collinson, M. M.; Wang, H. M.; Makote, R.; Khramov, A. *J. Electroanal. Chem.* **2002**, *519*, 65–71.
(17) Takahashi, H.; Li, B.; Sasaki, T.; Miyazaki, C.; Kajino, T.; Inagaki, S. *Chem. Mater.* **2000**, *12*, 3301–3305.
(18) Kirkor, E. S.; Scheeline, A. *J. Phys. Chem. B* **2001**, *105*, 6278–6280.
(19) Lei, C.; Shin, Y.; Liu, J.; Ackerman, E. J. *J. Am. Chem. Soc.* **2002**, *124*, 11242–11243.
(20) Jia, W. Z.; Wang, K.; Zhu, Z. J.; Song, H. T.; Xia, X. H. *Langmuir* **2007**, *23*, 11896–11900.
(21) Li, Y.; Jia, W. Z.; Song, Y. Y.; Xia, X. H. *Chem. Mater.* **2007**, *19*, 5758–5764.
(22) Li, Y.; Song, Y. Y.; Yang, C.; Xia, X. H. *Electrochem. Commun.* **2007**, *9*, 981–988.

10.1021/ac802739h CCC: $40.75
Published on Web 04/08/2009

and faster. Moreover, GOD entrapped in the matrix still retains its activity and does not incline to leak from the network. However, alcohol is involved in the process and the enzyme might be denatured (see Supporting Information, Figure S1).

As alcohol is a main concern in the sol−gel process when it is applied in bioencapsulation, some researchers have undertaken to solve this problem.[9,10] Take a sodium silicate process for example,[23,24] it involves two steps and releases a high concentration of Na^+, so an acidic cation-exchange resin has to be used to eliminate Na^+. Another method is to use glyceryl silicate[7] to provide mild encapsulation conditions. However, glyceryl silicate precursors should be synthesized first, which makes the process complicated. A third method is to use rotavaporization to remove alcohol.[25] A precursory sol solution is prepared first and rotavapor methods are used to eliminate ethanol. Then, enzymes could be added to the alcohol-free sol. This method is still time-consuming and complex.

In this study, we report a simple alcohol-free sol−gel approach to obtain a porous sol−gel silica matrix with horseradish peroxidase (HRP) entrapped in through an aqueous process by a one-step method. A buffer solution of HRP is mixed with a solution of ammonium hexafluorosilicate ($(NH_4)_2SiF_6$) to form a precursory sol solution. Application of a cathodic current to a working electrode leads to the reduction of water and the production of a hydrogen bubble dynamic template, which eventually results in the formation of a porous silica matrix catalyzed by the electrochemically formed hydroxyl ions at the electrode surface. The specific mechanism will be discussed in the following sections. Results show that such an aqueous sol−gel process combined with electrochemical inducement and hydrogen bubble template can obtain silica matrix with interconnected porous network structures as we expected. In addition, this is a highly controllable process. Such structures will facilitate the easy diffusion of small molecules of substrates of enzymes through the gel. Also, the encapsulated HRP through the aqueous route retains its functionalities, structural integrity, and stability because of the absence of alcohol. This newly developed protocol is simpler and faster and will certainly find extensive applications in biocatalysis, biosensors, bioelectronics, and biofuel cells.

EXPERIMENTAL SECTION

Chemicals and Materials. Horseradish peroxidase (HRP P8375 E.C. 1.11.1.7 RZ~3 activity~254 units/mg) was purchased from Sigma-Aldrich. All other chemicals were of analytical grade and were used without further purification, including ammonium fluorosilicate ($(NH_4)_2SiF_6$). Solutions of HRP and ammonium fluorosilicate were prepared using a 1.0 M ammonium acetate (CH_3COONH_4) buffer solution containing 0.1 M NH_4Cl (pH 7.0). Phosphate buffer solution (PBS; pH 7.4; containing 0.1 M KCl) was prepared by mixing stock solutions of KH_2PO_4 and K_2HPO_4. Solutions of hydrogen peroxide (H_2O_2) and hydroquinone (HQ) were prepared freshly using PBS. Ultrapure grade water (Milli-Q Millipore, U.S.A.) was used throughout the experiments.

Electrodeposition of HRP Sol−Gel Silica on a Au Electrode. The electrodeposition was carried out on an EG&G Galvanostate M273 (EG&G Princeton Applied Research). A traditional three-electrode system with a gold disk electrode (radius 3.0 mm) as the working electrode, a platinum wire (radius 0.5 mm, length 50 mm) as the auxiliary electrode, and a saturated calomel electrode (SCE) as the reference was applied.

The Au disk electrode was polished with 1.0, 0.3, and 0.05 μm alumina powders consecutively to get a mirror-like surface and then sonicated in water for 5 min. Prior to use, the electrode was electrochemically pretreated by cycling the potential from −0.2 to +1.6 V in a 0.5 M H_2SO_4 solution at the scan rate of 0.10 V s^{-1} to get a stable voltammogram.

A constant cathodic current of 0.0118 A (current density of 0.042 A cm^{-2}) was applied to the well pretreated gold disk electrode. The electrolyte was consisted of 0.15 M $(NH_4)_2SiF_6$ and 0.17 mg mL^{-1} HRP. After the electrochemical deposition, the modified electrode was rinsed thoroughly with ultrapure grade water and then soaked in PBS at 4 °C.

Instruments. Scanning electron microscopy (SEM) images were obtained from a Hitachi S3400 and S4800 scanning electron microscope (Hitachi, Japan). The FTIR spectra were collected on a Bruker TENSOR 27 spectrometer (Bruker, Germany) equipped with a liquid nitrogen cooled mercury−cadmium−telluride (MCT) detector. The UV−vis spectra were performed on a UV-3600 UV−vis spectrometer (Shimadzu, Japan).

The negative feedback mode and generation/collection mode of scanning electrochemical microscopy (SECM, CHI-900, CH Instrument Corp.) were used to get the approach curve and the distribution of HRP in the silica matrix, respectively. A three electrode system including a 10 μm Au disk microelectrode (purchased from CH Instrument) as the tip electrode, an Ag/AgCl (saturated KCl) electrode as the reference, and a platinum wire as the auxiliary electrode was used. The approach curve was recorded to adjust an appropriate tip-to-sample distance, and 10 mM solution of $K_3[Fe(CN)_6]$ was used as the redox species. Then, the sample-generation-tip-collection mode was performed to obtain the distribution of HRP through detecting the enzyme activity, and the electrolyte solution was PBS containing hydrogen peroxide (H_2O_2) and hydroquinone (HQ).

Other electrochemical experiments were carried out on a CHI 830 (CH Instrument corp., U.S.A.) electrochemical workstation. All the solutions of H_2O_2 and HQ were prepared with PBS (pH 7.4). A conventional three-electrode system with a HRP-encapsulated silica film electrode as the working electrode, a platinum wire (radius 0.5 mm, length 50 mm) as the auxiliary electrode, and a saturated calomel electrode (SCE) as the reference was used throughout. The differential pulse voltammetric measurements were taken in an unstirred electrochemical cell. Time-current curves were obtained by adding a standard solution of H_2O_2 and HQ after achieving a steady-state current. To eliminate dissolved oxygen, all the solutions used above were bubbled by highly pure nitrogen for 15 min, and then the nitrogen atmosphere was kept over the solutions through the experiments.

(23) Bhatia, R. B.; Brinker, C. J.; Gupta, A. K.; Singh, A. K. *Chem. Mater.* **2000**, *12*, 2434–2441.
(24) Yu, D.; Volponi, J.; Chhabra, S.; Brinker, C. J.; Mulchandani, A.; Singh, A. K. *Biosens. Bioelectron.* **2005**, *20*, 1433–1437.
(25) Ferrer, M. L.; del Monte, F.; Levy, D. *Chem. Mater.* **2002**, *14*, 3619–3621.

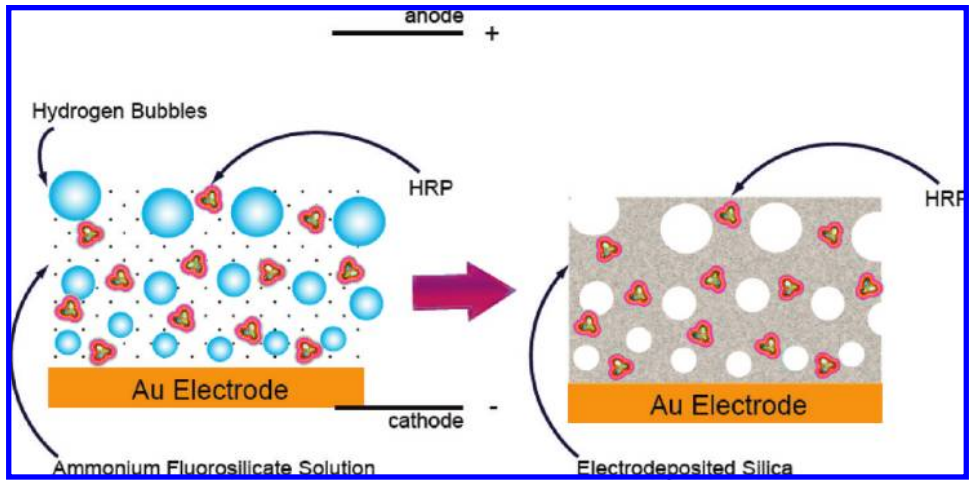

Figure 1. Illustration of the experimental procedure generating electrodeposited porous silica matrix.

RESULTS AND DISCUSSION

Structure of the Deposited Silica Matrix. The mechanism of electrochemically induced formation of silica can be described as follows:[26]

$$2H_2O + 2e \rightarrow 2OH^- + H_2 \quad (1)$$

$$SiF_6^{2-} + 4OH^- \rightleftharpoons Si(OH)_4 + 6F^- \quad (2)$$

$$Si(OH)_4 \rightarrow SiO_2 + 2H_2O \quad (3)$$

When a cathodic current is applied to the gold working electrode, water molecules are electrochemically reduced to hydroxyl ions and hydrogen bubbles (Figure 1). On one hand, the hydroxyl ions produced at the electrode surface catalyze the hydrolysis of SiF_6^{2-} to $Si(OH)_4$ then finally to silica. If biomolecules coexist with the silica precursor electrolyte, they can be entrapped in the silica matrix in situ. On the other hand, the generated hydrogen bubbles are critical in forming three-dimensional (3D) porous silica matrix. Figure 2 shows the surface morphology of the silica films for different times deposited at 0.042 A cm^{-2} from a 3 mL NH_4Ac buffer solution containing 0.15 M $(NH_4)_2SiF_6$. For comparison, the SEM image of a polished gold electrode is also presented (Figure 2a), which only shows scratches on the surface. After deposition of silica for 30 s, bright particles of silica regularly distributing on the electrode surface can be observed (Figure 2b). As time goes by, the particles aggregate into clusters and small particles still keep forming (Figure 2c). When electrodeposition duration continues to 300 s (Figure 2d), the entire electrode surface has been covered by silica film. Round holes of hydrogen bubbles can be clearly seen in the film. Besides, much smaller cavities interconnected by silica nanowires spread all over the relatively flat areas (Figure 2d, inset). This is because hydrogen bubbles have viscous force with silica, which confines silica to deposit along the gas/liquid interface and eventually results in the 3D porous, interconnected, and network-like structure. Such structure facilitates mass access, making substrate transport effective, and can release the inner stress of the silica film, avoiding phase cracking. However, if the

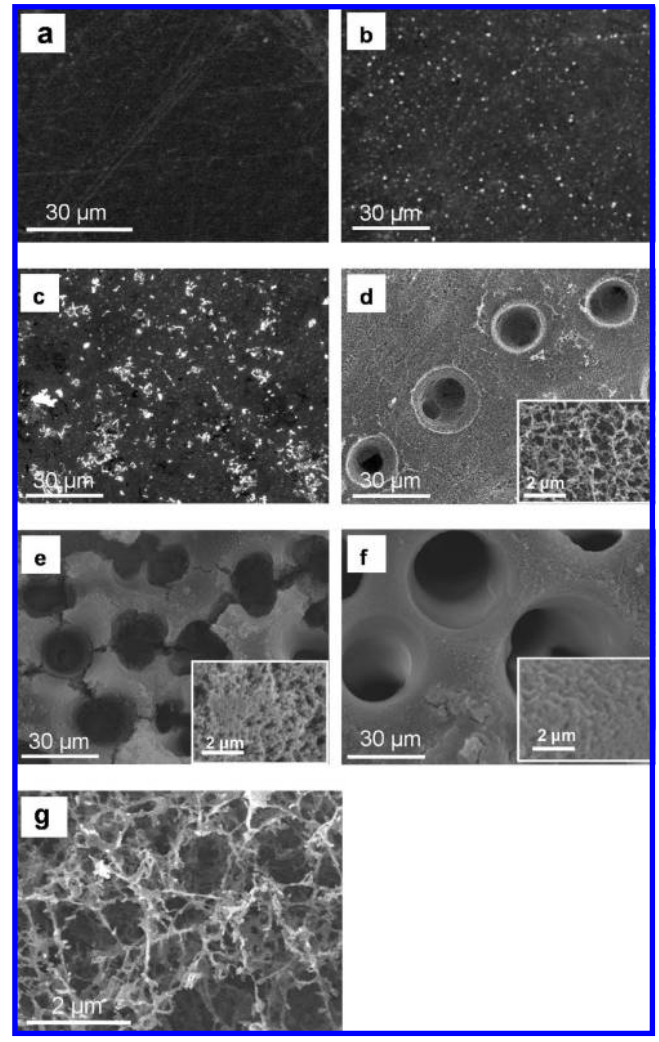

Figure 2. SEM images of silica film structures on Au electrode surface fabricated by electrolysis at 0.042 A cm^{-2} from a 3 mL of NH_4Ac buffer solution containing 0.15 M $(NH_4)_2SiF_6$ for 0 s (a), 30 s (b), 120 s (c), 300 s (d), 600 s (e), 1200 s (f), and 3 mL of NH_4Ac buffer solution containing 0.15 M $(NH_4)_2SiF_6$ and 0.17 mg/mL HRP for 300 s (g). Insets show the magnification of the flat areas of 300, 600, and 1200 s, respectively.

(26) Chigane, M.; Ishikawa, M.; Izaki, M. *Electrochem. Solid State Lett.* **2002**, *5*, D9−D12.

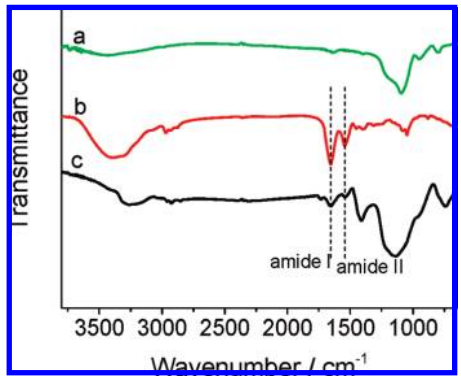

Figure 3. FTIR spectrum of a silica film (a), pure HRP (b), and HRP-encapsulated silica film (c).

deposition time lasts longer, for example, 600 s (Figure 2e), phase cracking occurs. The inset in Figure 2e shows that the structure of silica matrix becomes much denser, which influences the mass transport and has poor ability in releasing the inner stress effectively as well. Besides, more hydrogen bubbles are formed and likely to coalesce, resulting in enlarged hydrogen bubbles. Thus, during the evaporation of solvent, phase cracking caused by the inner stress gradient will occur. However, when the deposition time increases to 1200 s, silica deposited among the gap of bubbles becomes even denser than that of 600 s (Figure 2f, inset); therefore, the walls are thicker enough to sustain the porous structure and resist phase cracking when the silica film is dried. In addition, because of the hydrogen bubbles' coalescence, holes caused by those bubbles turn much larger. Silica films deposited on different electrodes for certain time, and repeatable morphologies can be achieved. The thickness of silica layer was estimated on a single-wavelength ellipsometry GES-5 (SOPRA) with a He−Ne laser light source (λ = 632.8 nm) at an incidence angle of 75°. It is found that the thickness of the silica matrix increases with the deposition time at an increasing rate of approximately 1.37 nm per second (see Supporting Information, Figure S2).

Taking the consideration of film stability and porous structure for mass transport, the silica film (ca. 400 nm thick) deposited for 300 s is ideal for biosensors fabrication, which will be used in the following experiments. Existence of HRP in the silica precursor solution does not alter the interconnected and network silica structures (Figure 2g). The enzyme is not distinguishable from the SEM image, which may imply that HRP molecules are encapsulated uniformly in the silica nanostructures. This is a clear advantage over the adsorption method which usually results in clustering of biomolecules on the silica films.[27]

FT-IR and UV−vis Characterizations. Pure silica films and HRP-encapsulated silica films deposited for 300 s have been characterized by FTIR (Figure 3). Curve a shows the FTIR absorption of a pure silica film. The broadband around 3400 cm^{-1} is due to the silanol group stretching vibration,[28] and the wide absorption band ranging from 1000−1300 cm^{-1} is attributed to the asymmetric stretching vibration mode of the Si−O−Si

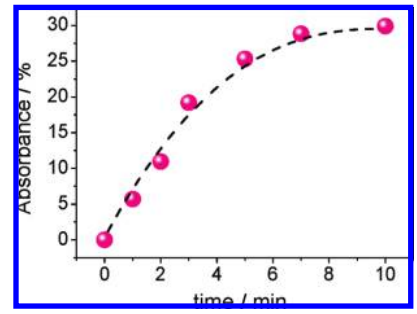

Figure 4. Loading density of HRP in the silica matrix as a function of electrodeposition time at 0.042 A cm^{-2} from a solution containing 0.15 M $(NH_4)_2SiF_6$ and 0.17 mg/mL HRP.

group.[13] Besides, the peak at approximately 800 cm^{-1} is also observed because of the symmetric stretching mode.[13] The absorption band around 1700−1600 cm^{-1} is amide I, attributed to the C=O stretching vibration of peptide linkage in the background of protein, and the absorption around 1625−1500 cm^{-1} is amide II, attributed to and N−H bending and C−N stretching. The protein secondary structure can be reflected through the positions of amide I and II bands in IR spectra. The characteristic absorption of amide I (1656 cm^{-1}) and amide II band (1542 cm^{-1}) can be seen from the spectrum of HRP-encapsulated silica film (Figure 3, curve c). There is no change of band positions as compared to the IR spectrum of pure HRP (Figure 3, curve b). This result indicates that HRP can retain its essential feature in the silica matrix, that is, HRP still keeps its secondary structure during the electrodeposition process. The peak at 1409 cm^{-1} is due to the adsorbed acetate ions on the electrode.[29,30]

To determine the loading density of HRP in the silica matrix, UV−vis spectrophotometry was taken. The absorbance of an electrolyte containing 0.15 M $(NH_4)_2SiF_6$ and 0.17 mg/mL HRP is first recorded before electrodeposition, and the characteristic Soret band at 403 nm can be observed. Then, the absorbance of the remaining electrolyte solution is collected after different deposition duration. It is observed that the absorbance at 403 nm keeps falling. As deposition time lasts, more HRP will be entrapped in the silica matrix and less HRP remains in the electrolyte solution; thus, the absorbance becomes smaller. The subtraction of absorbance from the value before deposition represents the loading density of HRP encapsulated in the silica matrix. In these experiments, the absorbance of electrolyte before electrodeposition is recorded as A_0. After electrodeposition, the absorbance of the rest electrolyte is recorded as A_n. Then, the value $(A_0 - A_n)/A_0$ represents the loading density of HRP encapsulated in silica at the electrode surface. The results are shown in Figure 4. In the first 420 s, the loading density of HRP on the electrode surface increases rapidly. Obviously, the longer the electrodeposition time is, the more HRP will be entrapped in the silica film. As HRP keeps being entrapped in the silica matrix, the concentration of HRP in the remaining electrolyte will decrease. When the deposition increases further (longer than 420 s), the amount of HRP in the silica matrix hereby

(27) Liu, A. L.; Zhou, T.; He, F. Y.; Xu, J. J.; Lu, Y.; Chen, H. Y.; Xia, X. H. *Lab Chip* **2006**, *6*, 811–818.
(28) Barranco, A.; Yubero, F.; Cotrino, J.; Espinos, J. P.; Benitez, J.; Rojas, T. C.; Allain, J.; Girardeau, T.; Reviere, J. P.; Gonzalez-Elipe, A. R. *Thin Solid Films* **2001**, *396*, 9–15.
(29) Farias, M. J. S.; Camara, G. A.; Tanaka, A. A.; Iwasita, T. *J. Electroanal. Chem.* **2007**, *600*, 236–242.
(30) Xia, X. H.; Liess, H. D.; Iwasita, T. *J. Electroanal. Chem.* **1997**, *437*, 233–240.

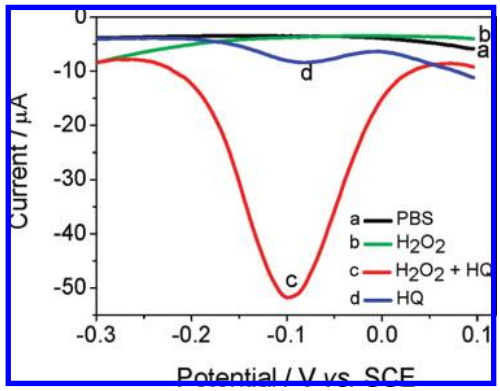

Figure 5. Differential pulse voltammograms of an HRP-SiO_2-modified Au electrode in solutions of pH 7.4 PBS containing 0 (a), 0.95 mM H_2O_2 (b), 0.95 mM H_2O_2 + 2 mM HQ (c), and 2 mM HQ (d). Pulse amplitude was 50 mV. The modified electrode was fabricated by electrolysis at 0.042 A cm^{-2} from 3.0 mL NH_4Ac buffer solution containing 0.15 M $(NH_4)_2SiF_6$ and 0.17 mg/mL HRP for 300 s.

increases slightly. Higher loading of biomolecules in silica films can be further achieved if higher concentration of the biomolecules in solution is used.

Electrochemical Characterization of the Bioactivity of HRP Encapsulated in the Silica Matrix. Figure 5 shows the differential pulse voltammograms of a Au electrode modified with HRP-encapsulated silica matrix in a solution of PBS. In the absence of H_2O_2 and HQ, there is no redox response of the HRP-SiO_2-modifed electrode besides a low background current (curve a). When 2 mM HQ is added, a reduction peak corresponding to the redox of HQ (curve d) appears. While only H_2O_2 exists, the HRP-silica-modified electrode has little response at potentials negative to −0.1 V because of the reduction of hydrogen peroxide at the uncovered gold electrode surface (curve b). When both H_2O_2 and HQ are present in solution, a considerable reduction peak appears (curve c), indicating that the encapsulated HRP in the silica matrix sustains its activity and HQ serves as an effective mediator of shuttling electrons between the electrode surface and the redox center of HRP. First, the redox center of HRP (Red) at its reducing state catalytically reduces H_2O_2 into H_2O, and HRP (Red) itself will turn into its oxidizing state HRP (Ox). Then, HQ can reverse HRP (Ox) back into HRP (Red) and be oxidized into benzoquinone (BQ). BQ can exchange electrons with the electrode, which electrochemically produces HQ. Therefore, HQ recycles in the system, leading to the increase of the reduction current. The specific reaction mechanism is as follows:

$$H_2O_2 + HRP(Red) \rightarrow HRP(Ox) + H_2O \quad (4)$$

$$HRP(Ox) + HQ \rightarrow BQ + HRP(Red) \quad (5)$$

$$BQ + 2H^+ + 2e \rightarrow HQ \quad (6)$$

The distribution of HRP in the silica matrix can be imaged by scanning electrochemical microscope (SECM). The negative feedback mode was used to get the approach curve with ferricyanide as the electrochemical probe. The final tip-to-substrate distance was 10 μm. Then, ferricyanide was replaced by H_2O_2 and HQ (The electrolytic cell was carefully rinsed before changing solutions). Substrate-generate-tip-collect mode was employed to get the SECM images (Figure 6). It can be observed that the current response to the HRP-SiO_2-modified electrode is about 30 times as large as that to the SiO_2-modified electrode. This is due to the catalytic ability of HRP as described in reactions 4−6. Besides, the current range is narrow. Since a high current response corresponds to the area with HRP of a relatively high concentration, it can be seen that HRP uniformly distributes in the silica matrix from Figure 6b.

It is known that pH influences the conformation of the enzyme and its bioactivity. Silica matrix can protect the entrapped enzyme from being damaged by detrimental substances and provide a biocompatible microenvironment, which can help the enzyme to retain its bioactivity and conformation. Figure 7 shows the comparison of pH effect on HRP encapsulated in the silica matrix and HRP physically adsorbed in the silica matrix. It shows that both the encapsulated and the adsorbed HRP exhibit best activity in the solution of pH 7.4. At other solution pH values, the bioactivity of the physically adsorbed HRP decreases much faster than the encapsulated one. For example, in the solution of pH 4.5, the encapsulated HRP still remains 72% of the activity in the solution of 7.4, whereas the adsorbed HRP remains 43% only. When HRP molecules are encapsulated in a silica matrix, they are surrounded by silica network, which serves like a "shell" protecting them from being disturbed by the outer environment.

All of the above taken measures of the electrochemistry demonstrate that the HRP encapsulated in the silica matrix has outstanding performance in the catalytic reduction of H_2O_2. Silica matrix derived through this method does provide a biocompatible environment to HRP.

Amperometric Response and Calibration Curve. Figure 8 shows the effect of working potential on the steady-state current of the encapsulated HRP-SiO_2/Au electrode. The current increases dramatically with working potential altering from −0.05 V to −0.15 V and then levels off afterward. Therefore, the detection potential of −0.2 V was selected to ensure a relatively high sensitivity, sufficient current response, as well as relatively low background current of the present biosensor.

At the working potential of −0.2 V, H_2O_2 and HQ were regularly added into the stirred PBS (pH 7.4) to obtain the typical steady-state current−time plot (Figure 9). It is obvious that the reduction current increases sharply to reach a stable value within 5 s by each addition. Such a quick response can be attributed to the interconnected porous structure of silica matrix which does not inhibit mass transport. Figure 10 shows the corresponding calibration curve between amperometric current and H_2O_2 concentration. The linear response range is from 0.02 to 0.20 mM with a correlation coefficient of 0.9934 and a detection limit of 3 μM at a signal-to-noise ratio of 3. The current−time response curve indicates that the process follows a typical Michaelis−Menten process. The apparent Michaelis−Menten constant (K_M^{app}), considered to be the characteristics of enzyme reaction kinetics, can be calculated from the Lineweaver−Burk equation.[31] The constant is estimated to be 0.88 mM, which is larger than the value of free HRP mol-

(31) Deng, Y. J.; Shi, J. B.; Jiang, L. X.; Gao, J.; Yao, Q. Z. *Acta Chim. Sinica* **2006**, *64*, 1911–1915.

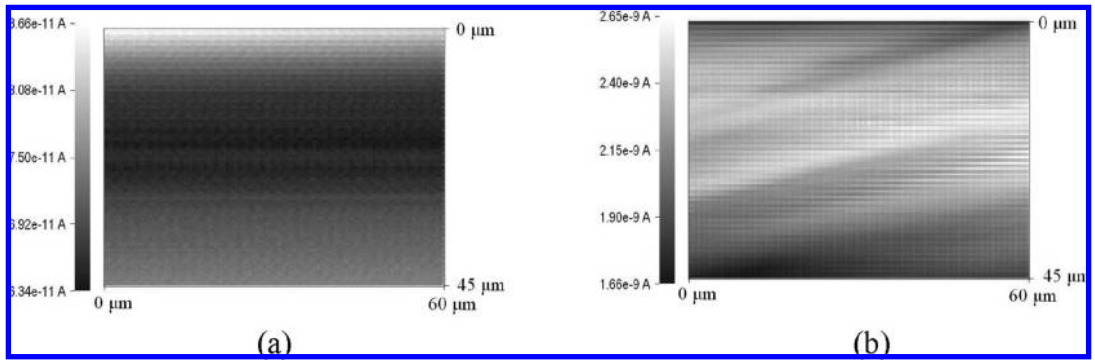

Figure 6. SECM images of a SiO_2-modified Au electrode (a), HRP- SiO_2-modified Au electrode (b) in a solution of 0.4 mM HQ and 0.4 mM H_2O_2 at a scan rate of 30 μm/s with the gold tip potential of −0.2 V vs Ag/AgCl. The conditions of electrodeposition were the same as in Figure 5.

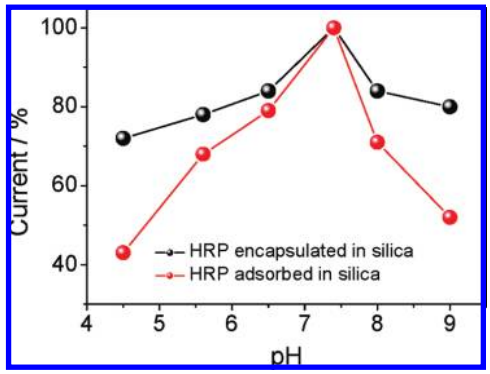

Figure 7. Effect of solution pH on the electrocatalytic responses of the encapsulated-HRP-silica-modified electrode (solid black circle) and physically adsorbed-HRP-silica-modified electrode (solid red circle) at −0.2 V to PBS containing 0.2 mM H_2O_2 and 0.2 mM HQ. The encapsulated-HRP-silica-modified electrode was fabricated by electrolysis at 0.042 A cm^{-2} from 3.0 mL NH_4Ac buffer solution containing 0.15 M $(NH_4)_2SiF_6$ and 0.17 mg/mL HRP for 300 s. The physically adsorbed-HRP-silica-modified electrode was fabricated by electrolysis at 0.042 A cm^{-2} from a 3.0 mL NH_4Ac buffer solution containing 0.15 M $(NH_4)_2SiF_6$ for 300 s, then immersing in the 0.17 mg/mL HRP solution for 24 h.

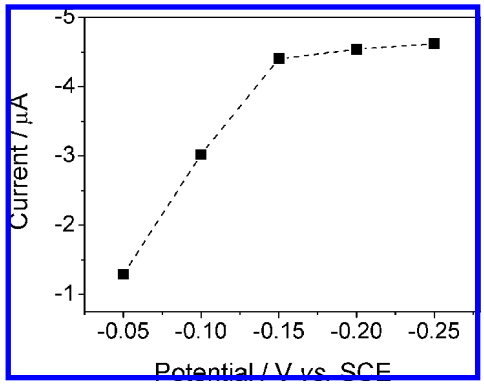

Figure 8. Effect of the working potential on the response of the encapsulated HRP- SiO_2-modified Au electrode to pH 7.4 PBS containing 0.2 mM H_2O_2 and 0.2 mM HQ. The modified electrode was fabricated by electrolysis at 0.042 A cm^{-2} from 3.0 mL NH_4Ac buffer solution containing 0.15 M $(NH_4)_2SiF_6$ and 0.17 mg/mL HRP for 300 s.

ecules,[32] resulting from the diffusional resistance.[23] However, this value is much smaller than the ones from other sol−gel methods.[33,34] Apparently, the encapsulated HRP by the present

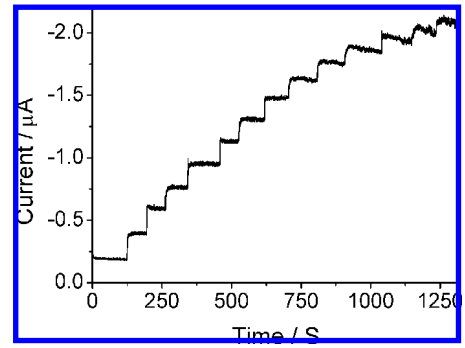

Figure 9. Typical current−time response curves of a HRP- SiO_2-modified Au electrode upon successive addition of 0.02 mM H_2O_2 and 0.02 mM HQ at an applied potential of −0.2 V. The modified electrode was fabricated by electrolysis at 0.042 A cm^{-2} from 3.0 mL of NH_4Ac buffer solution containing 0.15 M $(NH_4)_2SiF_6$ and 0.17 mg/mL HRP for 300 s.

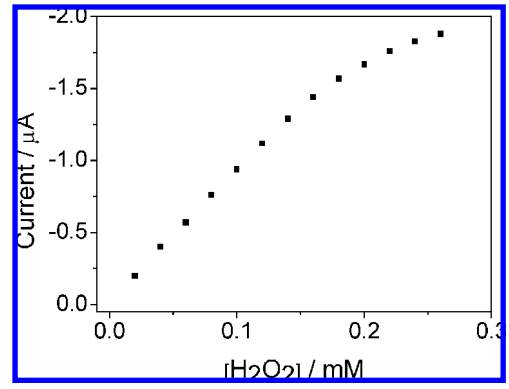

Figure 10. Relationship between the concentration of H_2O_2 and response current.

method exhibits high biocatalytic activity toward the reduction of H_2O_2, which is quite probable because of high affinity of the encapsulated HRP to its substrate and the fast mass transport of analytes and products as well.

Stability of the Encapsulated HRP. The stability of HRP encapsulated in the silica matrix through our alcohol-free process

(32) Gilabert, M. A.; Fenoll, L. G.; Garcia-Molina, F.; Tudela, J.; Garcia-Canovas, F.; Rodriguez-Lopez, J. N. *Biol. Chem.* **2004**, *385*, 795–800.
(33) Yu, J. H.; Ju, H. X. *Anal. Chem.* **2002**, *74*, 3579–3583.
(34) Chen, H. J.; Dong, S. J. *Biosens. Bioelectron.* **2007**, *22*, 1811–1815.

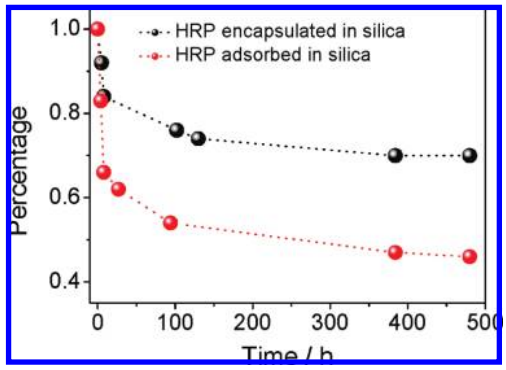

Figure 11. Stability of HRP determined in a solution of pH 7.4 PBS containing 0.2 mM H_2O_2 and 0.2 mM HQ with a potential of −0.2 V. (solid black circles) HRP encapsulated in the silica matrix; (solid red circles) HRP physically adsorbed in the silica matrix. The encapsulated-HRP-silica-modified electrode was fabricated by electrolysis at 0.042 A cm^{-2} from 3.0 mL of NH_4Ac buffer solution containing 0.15 M $(NH_4)_2SiF_6$ and 0.17 mg/mL HRP for 300 s. The physically adsorbed-HRP-silica-modified electrode was fabricated by electrolysis at 0.042 A cm^{-2} from 3.0 mL NH_4Ac buffer solution containing 0.15 M $(NH_4)_2SiF_6$ for 300 s and then immersing in the 0.17 mg/mL HRP solution for 24 h.

was examined, with the results shown in Figure 11. Within the first 8 h, the current response decreases dramatically and tends to reach steady state after 12 h. After 480 h storage in PBS at 4 °C, the enzyme still maintains 70% of its initial response. In comparison, HRP physically adsorbed in the silica matrix only retains 46% of its original response after being stored in PBS at 4 °C for 480 h. Such a huge difference may be caused by the different situations of the HRP through different immobilization methods. Silica matrix can provide the encapsulated HRP a sheltered environment that can both keep the secondary structure of enzyme and avoid leakage from the matrix since silica may have a mild yet sufficiently strong interaction with the enzyme. However, the desorption of HRP by physical adsorption cannot be kept from happening, which leads to the relatively greater loss of activity.

CONCLUSIONS

An electrochemically induced alcohol-free sol−gel process to obtain 3D porous silica matrixes was presented. Hydrogen bubbles were involved in the process to assist forming a porous structure. The present method is a quick, simple, low-cost process, and the present directed assembly can be controlled spatially and temporally. Results showed that the formed silica matrixes had uniform porous structures which could provide a biocompatible environment to biomolecules, facilitate mass transport, and enhance the mechanical stability of the matrixes. The biomolecule, HRP, exhibited high bioactivity and retained its secondary structure. This method can be applied to mediate the assembly of biomoelcules and additional components (e.g., nanoparticles and proteins) and provides a promising approach for fabricating biosensors with the immobilization of a variety of biomolecules.

ACKNOWLEDGMENT

This work was supported by the National Basic Research Program (2007CB714501, 2007CB936404), the National Natural Science Foundation of China (20535010, 20775035, 20828006), the National Science Fund for Creative Research Groups (20521503).

SUPPORTING INFORMATION AVAILABLE

Further details are given as noted in the text and in Figures S1 and S2. This material is available free of charge via the Internet at http://pubs.acs.org.

Received for review December 25, 2008. Accepted March 27, 2009.

AC802739H